Drosophila TIMP Is a Potent Inhibitor of MMPs and TACE: Similarities in Structure and Function to TIMP-3[†]

Shuo Wei, Zhihong Xie, Elena Filenova, and Keith Brew*

Department of Biomedical Sciences, Florida Atlantic University, Boca Raton, Florida 33431

Received July 31, 2003; Revised Manuscript Received September 4, 2003

ABSTRACT: The four tissue inhibitors of metalloproteinases (TIMPs) are endogenous inhibitors that regulate the activity of matrix metalloproteinases (MMPs) and certain disintegrin and metalloproteinase (ADAM) family proteases in mammals. The protease inhibitory activity is present in the N-terminal domains of TIMPs (N-TIMPs). In this work, the N-terminal inhibitory domain of the only TIMP produced by *Drosophila* (dN-TIMP) was expressed in *Escherichia coli* and folded *in vitro*. The purified recombinant protein is a potent inhibitor of human MMPs, including membrane-type 1-MMP, although it lacks a disulfide bond that is conserved in all other known N-TIMPs. Titration with the catalytic domain of human MMP-3 [MMP-3(ΔC)] showed that dN-TIMP prepared by this method is correctly folded and fully active. dN-TIMP also inhibits, *in vitro*, the activity of the only two MMPs of *Drosophila*, *dm1*- and *dm2*-MMPs, indicating that the *Drosophila* TIMP is an endogenous inhibitor of the *Drosophila* MMPs. dN-TIMP resembles mammalian N-TIMP-3 in strongly inhibiting human tumor necrosis factor-α-converting enzyme (TACE/ADAM17) but is a weak inhibitor of human ADAM10. Models of the structures of dN-TIMP and N-TIMP-3 are strikingly similar in surface charge distribution, which may explain their functional similarity. Although the gene duplication events that led to the evolutionary development of the four mammalian TIMPs might be expected to be associated with functional specialization, *Timp-3* appears to have conserved most of the functions of the ancestral TIMP gene.

The matrix metalloproteinases (MMPs)[1] are secreted or membrane-bound proteases that catalyze the turnover of extracellular matrix (ECM) components (*1*, *2*). The ADAM (a disintegrin and a metalloproteinase) family proteases are cell surface proteins with adhesive and/or protease activity (*3*). Proteolytically active members of these two families share a common zinc-binding motif (HEXXHXXGXXH) and a Met turn so both are members of the "metzincin" superfamily (*4*). Abnormal MMP or ADAM activities are linked to diseases such as cancers and arthritis (*1*, *5*).

The tissue inhibitors of metalloproteinases (TIMPs) are endogenous proteins that regulate the activity of MMPs through direct inhibition or by modulating zymogen activation (*6*). In mammals, the TIMP family consists of four members, TIMP-1−TIMP-4, and their inhibitory activities toward different MMPs are not particularly specific (*6*), although TIMP-1 is a very weak inhibitor for MT-MMPs as compared with the other TIMPs (*7*−*10*). Recently, TIMP-3 was found *in vitro* to inhibit the activities of some members of the ADAM and ADAMTS (a disintegrin and metalloproteinase with thrombospondin type 1 domain) families, including ADAM10 (*11*), ADAM12-S (*12*), TACE (TNF-α-converting enzyme)/ADAM17 (*13*), ADAMTS-4, and ADAMTS-5 (*14*, *15*). The apparent K_i values of these inhibitory interactions are in the sub-nanomolar range, and the interactions are primarily through the association of the N-terminal domain of TIMP-3 with the metalloproteinase domains of ADAMs and ADAMTSs (*15*−*17*). Among the other TIMPs, only TIMP-1 has a high level of inhibitory activity for an ADAM, with an apparent K_i for ADAM10 of 0.1 nM (*11*).

TIMP genes are also present in invertebrates, such as *Drosophila melanogaster* (*18*), *Caenorhabditis elegans* (*6*), and *Caenorhabditis gigas* (*19*). Interestingly, the *Drosophila* synapsin and TIMP genes have nested exon−intron structures that are very similar to those of the three synapsin genes and genes encoding TIMP-1, -3, and -4 in humans, suggesting a highly conserved genomic organization within this locus (*18*, *20*, *21*). Unlike other currently known TIMPs, the N-terminal inhibitory domain of *Drosophila* TIMP lacks a disulfide bond corresponding to the Cys^{13}−Cys^{124} disulfide in human TIMP-1 (*6*). Disruption of *Timp* in *Drosophila* resulted in a subviable phenotype. Adult mutants exhibited inflated wings, bloated guts and tissue autolysis, and impaired phototactic responses and died prematurely (*22*). This phenotype suggests that in the *Timp* mutants, ECM turnover is imbalanced, cell−cell or cell−matrix adhesion is disrupted, and the nervous system is dysfunctional (*22*). Because TIMPs have a primary function as metalloproteinase inhibitors, it is reasonable to hypothesize that some aspects of the mutant phenotype result from disrupted regulation of metzincins.

[†] This work was supported by NIH Grant AR40994.

* To whom correspondence should be addressed. Telephone: (561) 297-0407. Fax: (561) 297-2519. E-mail: kbrew@fau.edu.

[1] Abbreviations: TIMPs, tissue inhibitors of metalloproteinases; MMPs, matrix metalloproteinases; dN-TIMP, N-terminal domain of the *Drosophila* tissue inhibitor of metalloproteinases; ADAM, a disintegrin and a metalloproteinase domain; ADAMTS, a disintegrin and a metalloproteinase domain with thrombospondin type 1 domains; TACE, TNF-α-converting enzyme; ΔC, C-terminally truncated; CD, catalytic domain; $K_i^{(app)}$, apparent inhibition constant.

10.1021/bi035358x CCC: $25.00
Published on Web 10/03/2003

Two MMP genes were discovered in *Drosophila* recently. The products of these two genes, *Dm1*-MMP and *Dm2*-MMP, are more closely related to the membrane-type MT-MMPs than to other vertebrate MMPs (*23*, *24*). Extensive searches of the *Drosophila* genome indicate that these are the only MMPs in this organism (*24*). Hynes and Zhao have identified seven ADAM and ADAMTS genes in *D. melanogaster* (*25*). Sequence comparisons of these genes with their vertebrate counterparts reveal that they encompass four ADAM genes (probable orthologues of mammalian ADAM9, -10, -12, and -17, respectively), two ADAMTS genes, and one unidentified gene with a sequence similar to those of mammalian ADAM10 and ADAM17. Among these genes, only the *Drosophila* Kuzbanian/ADAM10 gene has been characterized; this is a major component of the Notch signaling pathway (*26*, *27*) and has an important role in neurogenesis (*26*, *28*), wing development (*29*), and axonal extension (*30*). The function of *Drosophila* TIMP is likely to be related to regulation of the activities of some or all of these metalloproteinases.

This work was designed to investigate the activity of *Drosophila* TIMP as an inhibitor of *Drosophila* MMPs and other enzymes to provide a molecular basis for genetic studies of *Drosophila* metzincins and inhibitors. Previous studies have shown that bacterially expressed forms of the N-terminal domains of TIMPs can fold *in vitro* into the correct native structures that carry the inhibitory activities against the MMPs, ADAMs, and ADAMTSs (*15*, *16*, *31*, *32*). In this paper, we describe an *Escherichia coli* expression system for the N-terminal inhibitory domain of *Drosophila* TIMP (dN-TIMP). A His_8-tagged dN-TIMP was expressed in *E. coli* BL21(DE3) cells, purified, and folded *in vitro*. The recombinant protein inhibits both *Drosophila* MMPs as well as all human MMPs that have been tested, including the membrane-type MT1-MMP. dN-TIMP also inhibits both human TACE/ADAM17 and Kuzbanian/ADAM10. The properties of *Drosophila* TIMP suggest that it functions *in vivo* as an endogenous inhibitor of MMPs and ADAMs.

EXPERIMENTAL PROCEDURES

Materials. Vectors and cell lines for expression of dN-TIMP and the two *Drosophila* MMPs were from the same sources as in previous studies (*15*, *31*). Miniprep and gel extraction kits were purchased from Qiagen. Restriction enzymes and Vent PCR kits were obtained from New England BioLabs. The *Drosophila* cDNA clone for TIMP (GH26186) was from Research Genetics, and the *Drosophila* embryonic cDNA library was kindly provided by T. E. Haerry (Department of Biological Sciences, Florida Atlantic University). PCRs were performed using a PCR Sprint HYBAID system from Midwest Scientific. Primers were synthesized by Sigma Genosys, and DNA sequencing was performed in the laboratory of R. Werner (Department of Biochemistry and Molecular Biology, University of Miami School of Medicine, Miami, FL). Automated Edman degradation and mass spectrometry of dN-TIMP were carried out by J. Pohl (Winship Cancer Institute, Emory University School of Medicine, Atlanta, GA). The protease inhibitor cocktail (for bacterial cell extracts) was purchased from Sigma, while the sequencing grade modified trypsin was from Promega. The Biologic DuoFlow medium-pressure chromatography system was supplied by Bio-Rad, and the weak cation exchange Fractogel EMD COO^- PEEK column was from EM Separations Technology. Active forms of human MMP-1 and MMP-2 and catalytic domains of MMP-3 [MMP-3(ΔC)] and MT1-MMP [MT1-MMP(CD)] were gifts from H. Nagase (Kennedy Institute of Rheumatology, Imperial College of Science, Technology and Medicine, London, U.K.). N-TIMP-3 was prepared as described previously (*15*). The recombinant ectodomains of human TACE and ADAM10 were from R&D Systems. Synthetic fluorogenic peptide substrates Knight (Mca-Pro-Leu-Gly-Leu-Dpa-Ala-Arg-NH_2) and NFF-3 (Mca-Arg-Pro-Val-Glu-Nva-Trp-Arg-Lys-Dnp-NH_2) were purchased from Bachem, while Substrate III (Mca-Pro-Leu-Ala-Gln-Ala-Val-Dpa-Arg-Ser-Ser-Ser-Arg-NH_2) was from R&D Systems.

Construction of the dN-TIMP Bacterial Expression System. The gene encoding the N-terminal inhibitory domain of *Drosophila* TIMP (dN-TIMP, Cys^1—Asn^{117}) was directly amplified from *E. coli* strain DH5α carrying *Drosophila* cDNA clone GH26186 (ResGen). One colony was added to the PCR mixture and the mixture boiled for 10 min. Subsequently, Vent DNA polymerase was added, and the PCR was carried out for 30 cycles at 94 °C for 30 s, 60 °C for 30 s, and 72 °C for 1 min. An additional translation-initiating methionine (bold) together with an *Nde*I site (underlined) at the 5′-end and a *Not*I site (underlined) at the 3′-end were introduced by the primers 5′-AAAAAA-CAT**ATG**TGCAGCTGCATGCCATCTCAC-3′ (forward) and 5′-AAAAAAAGCGGCCGCATTGGTGGCCTTGG-CATA-3′ (reverse), respectively. The PCR product was cloned into the pET-42b vector using the *Nde*I and *Not*I sites to produce the coding sequence for dN-TIMP with a His_8 tag attached to the C-terminus.

Expression in E. coli and Folding of dN-TIMP. The plasmid pET-42b::*dN-Timp* was transformed into *E. coli* BL21(DE3) cells and expressed essentially as described for N-TIMP-3 (*15*). Purification and folding were carried out using a method similar to that previously developed for human N-TIMP-3 (*15*), except that 5 volumes of folding buffer was used in the folding procedure instead of 15 volumes, and the CM-52 cation exchange chromatography was carried out at pH 7.0 instead of pH 8.0 for N-TIMP-3. To further purify the dN-TIMP, the protein eluted from the CM-52 column was dialyzed overnight against 15 volumes of 20 mM Tris-HCl (pH 6.0) containing 20% glycerol and applied to a Fractogel EMD CM column previously equilibrated with the same buffer and connected to a Bio-Rad Biologic DuoFlow medium-pressure chromatography system. A linear salt gradient from 0 to 0.5 M NaCl was used to elute the bound protein. The inhibitory activity of different fractions against human MMP-1 was estimated using the fluorescence assay method with the Knight substrate. Fractions from the active peak were pooled and used to titrate 200 nM MMP-3(ΔC) as described below. The concentration of dN-TIMP was determined with the Bio-Rad dye binding protein assay kit using bovine serum albumin as a standard.

Determination of the Near- and Far-UV CD Spectra of dN-TIMP. Near- and far-UV CD spectra of recombinant dN-TIMP were recorded with a JASCO J-600 spectropolarimeter. The protein was dialyzed against 10 mM MES (pH 6.0) containing 50% glycerol, and 10 spectra were scanned at a rate of 50 nm/min at 30 °C. The spectra were averaged, and the baseline, determined with buffer alone, was subtracted.

Near-UV CD spectra (250−320 nm) were recorded at a protein concentration of 0.3 mg/mL using a cell with a path length of 1 cm, and far-UV spectra (200−250 nm) were recorded at a protein concentration of 0.15 mg/mL using a cell with a path length of 0.1 cm.

Cloning of dm1- and dm2-Mmp Genes and Construction of the Bacterial Expression System. The cDNAs for the two MMPs were derived from the *Drosophila* embryonic cDNA library. The primer pairs 5′-AAAAAACATATGCAATCGGCACCCGTTTCC-3′ (forward) and 5′-AAAAAAGGATCCTTACTAATACAGTGACTGGATGGC-3′ (reverse) and 5′-GGAATTCCATATGTTCGCCCTGCAGGGACCCAAGTGG-3′ (forward) and 5′-CGGGATCCTTACTAGTACAACTGCTGAATGCCATA-3′ (reverse) were used for amplifying *dm1*- and *dm2*-MMP genes (regions encoding the catalytic domains only), respectively. Additional translation start and stop codons (bold) were introduced together with *Nde*I and *Bam*HI restriction sites, respectively (underlined). PCRs were carried out for 50 cycles at 94 °C for 30 s, 65 °C for 30 s, and 72 °C for 1 min using the Vent PCR kit. The PCR product was cloned into the pET-3a vector using the *Nde*I and *Bam*HI sites to produce the coding sequence for the catalytic domains of *dm1*-MMP (with the pro peptide) and *dm2*-MMP (without the pro peptide).

Expression in E. coli and Folding of dm1- and dm2-MMPs. Plasmids pET-3a::*dm1-mmp* and pET-3a::*dm2-mmp* were transformed into *E. coli* BL21(DE3) cells separately. The proteins were expressed, and the bacterial cells were lysed as for dN-TIMP, except that 1 mL of protease inhibitor cocktail was added during the final washing of the inclusion bodies. The inclusion bodies were subsequently dissolved by stirring them overnight in 20 mM Tris-HCl (pH 8.5), 8 M urea, and 10 mM DTT. After centrifugation at 30 000 rpm for 20 min, the supernatant was applied to an anion exchange Q-50 column pre-equilibrated with 20 mM Tris-HCl (pH 8.0) containing 8 M urea, and the bound protein was eluted with a linear gradient from 0 to 0.5 M NaCl. The products were homogeneous on SDS−PAGE. The eluted protein was diluted to approximately 200 μg/mL with 20 mM Tris-HCl (pH 8.0) containing 8 M urea, and protease inhibitor cocktail (1 mL/13 mL of protein solution) was added. The solution was incubated for 2.5 h at room temperature and then dialyzed against two changes (16 h each) of 10 volumes of 50 mM Tris-HCl (pH 8.0) containing 250 mM NaCl, 20 mM $CaCl_2$, 0.02% Brij, 5 mM DTT, and 20% glycerol. The precipitate was removed by centrifugation at 30 000 rpm for 30 min at 4 °C. The supernatant, containing the folded enzyme, was stored at −80 °C.

MMP Inhibition Studies. The $K_i^{(app)}$ values of dN-TIMP against MMP-1, -2, and -3(ΔC) were determined using fluorescence assays as described previously for N-TIMP-1 mutants (*33*). The inhibitory activity for MT1-MMP(CD) was determined by incubating 5 nM enzyme with different concentrations of inhibitors for 4 h at room temperature and measuring the residual enzyme activity with 3 μM Knight substrate. For titration of dN-TIMP, 200 nM MMP-3(ΔC) was incubated with various concentrations of dN-TIMP (0−400 nM) at room temperature overnight. The samples were subsequently diluted 200-fold, and residual enzyme activity was immediately measured using 1.5 μM NFF-3.

For inhibition assays of *Drosophila* MMPs, 50 μM $ZnCl_2$ was first added to the enzyme solutions to introduce the catalytic activity. Pro-*dm1*-MMP was activated by adding trypsin to a mass ratio of 500:1 (MMP:trypsin) and incubated for 1 h at room temperature. Phenylmethanesulfonyl fluoride (PMSF) was then added in excess to completely inhibit the trypsin activity. The activated *dm1*-MMP was subsequently diluted to 10 nM and the active form of *dm2*-MMP to 100 nM in TNC buffer [50 mM Tris-HCl (pH 7.5), 150 mM NaCl, 10 mM $CaCl_2$, and 0.02% Brij 35]. The active enzyme solution was preincubated with different concentrations of dN-TIMP at room temperature for 2 h, followed by adding Knight substrate to a final concentration of 3 μM. The fluorescence intensity was measured every 30 min for 2 h in a Perkin-Elmer LS50B luminescence spectrometer.

ADAM Inhibition Kinetic Studies. dN-TIMP and N-TIMP-3 were diluted in assay buffer [25 mM Tris-HCl (pH 9.0), 2.5 μM $ZnCl_2$, and 0.005% Brij 35], and different concentrations of inhibitors were incubated with 0.14 nM recombinant human TACE ectodomain (70 kDa) or 19.2 nM recombinant human ADAM10 ectodomain (60 kDa). The incubation conditions for hTACE and hADAM10 were 4 h at room temperature and 1 h at 37 °C, respectively. Substrate III (R&D Systems) was then added to a final concentration of 10 μM, and kinetic assays were carried out at the same temperature as preincubation. The excitation and emission wavelengths used here were 320 and 405 nm, respectively. TACE activity is inhibited by NaCl (protocol from R&D Systems), and N-TIMPs were diluted more than 800-fold with assay buffer from the stock solution so that the final salt concentration was sufficiently low (well below 1 mM) that it did not interfere with the assay.

Homology Modeling of dN-TIMP and N-TIMP-3 Structures. The structural models of dN-TIMP and N-TIMP-3 were generated with a Silicon Graphics Indigo 2 workstation using the Homology module of the Insight II software package. Coordinates of these two N-TIMPs were assigned on the basis of the published crystal structures of TIMP-1 (*34*) and TIMP-2 (*35*) in complexes with MMPs. The original models were subsequently refined by molecular dynamics simulations for 500 cycles at 500 K and energy minimization (conjugate algorithm, 100 iterations, and derivative of 0.1). The electrostatic surface potentials were calculated and displayed using GRASP (*36*).

RESULTS

Production and Characterization of dN-TIMP. Comparison of the N-terminal inhibitory domains of four human TIMPs with dN-TIMP (*6*) shows that N-TIMP-3 is the one most similar to dN-TIMP (25% identical and 50% similar). dN-TIMP is also most similar to N-TIMP-3 in isoelectric point (9.42 as compared to 9.27), whereas the other three human N-TIMPs (N-TIMP-1, -2, and -4) are less cationic with pI values of 8.27, 6.98, and 7.18, respectively. Therefore, we used a purification and folding procedure for dN-TIMP similar to that previously developed for N-TIMP-3 (*15*).

Unfolded dN-TIMP (∼180 mg) was purified from 3 L of *E. coli* culture in the presence of 6 M guanidine hydrochloride using a Ni^{2+}−NTA affinity column. *In vitro* folding of 10 mg of unfolded protein yielded 1−1.5 mg of active dN-TIMP. Two protein peaks were eluted from the CM-52 column, but only the second peak had MMP inhibitory activity. The protein in this peak exhibited a single compo-

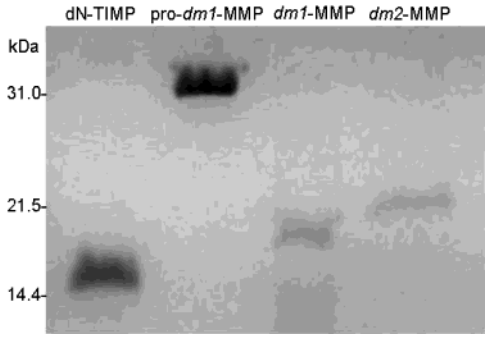

FIGURE 1: SDS−PAGE of the *Drosophila* TIMP and MMPs. From left to right: dN-TIMP (2 μg), inactive pro-*dm1*-MMP (4 μg), activated *dm1*-MMP (from 4 μg of pro enzyme), and active *dm2*-MMP (0.5 μg).

nent on SDS−PAGE under reducing conditions (Figure 1, lane 1).

Mass spectrometric analysis indicated the presence of a single molecular species with a mass of 14 864.7 kDa, in close agreement with the expected value of 14 863.9 kDa. Automated Edman degradation showed that the active protein has a single N-terminal sequence (X-S-X-M-P-S-H-P-Q-T-H-F-A), in exact agreement with the expected N-terminal sequence of mature dN-TIMP, if it is assumed that the unidentified amino acids (X) correspond to disulfide-bonded Cys residues which are not identified by this method. This result shows that the initiator methionine, added to facilitate expression in *E. coli*, is efficiently removed as in human N-TIMP-1 (*31*).

It has been reported previously that a fraction of N-TIMPs expressed in *E. coli* is inactive due to N-terminal acetylation, and the active and inactive forms can be separated using a medium-pressure chromatography system (refs *33*, *37*, and *38* and our unpublished data). However, dN-TIMP, prepared as described here, appears to be devoid of inactive subspecies. Unlike N-TIMP-3 (*15*), there is no significant difference in activity between the earlier and the later fractions of the active peak, and mass spectrometry does not show any peak corresponding to the N-acetylated form. Furthermore, titration of MMP-3(ΔC) with dN-TIMP showed that ~100% of the inhibitor is active (Figure 2).

The far-UV CD spectrum of dN-TIMP (Figure 3, left) is qualitatively similar to that of N-TIMP-1 (*31*), but the near-UV spectrum (Figure 3, right) is distinct, reflecting differences in the content and location of aromatic amino acids in dN-TIMP and N-TIMP-1. In particular, dN-TIMP is devoid of tryptophans, the single tryptophan of N-TIMP-1 (Trp^{105}) being replaced with Tyr in the *Drosophila* inhibitor.

Cloning and Expression of dm1- and dm2-MMPs. cDNAs encoding the catalytic domains of *dm1*-MMP (with the pro peptide) and *dm2*-MMP (without the pro peptide) were obtained from a *Drosophila* embryonic cDNA library; their sequences are identical to those reported by Llano *et al.* (*23*, *24*). Both were cloned into pET-3a vectors and expressed under the control of the T7 promoter in *E. coli*. The expressed protein was extracted from inclusion bodies, folded *in vitro* in the presence of Ca^{2+} but not Zn^{2+}, and purified to homogeneity (Figure 1, lanes 2 and 4). *dm1*-MMP was completely activated after treatment with trypsin, as suggested by the conversion of the pro enzyme to the 19 kDa active form (Figure 1, lane 3). The activity of *dm1*-MMP,

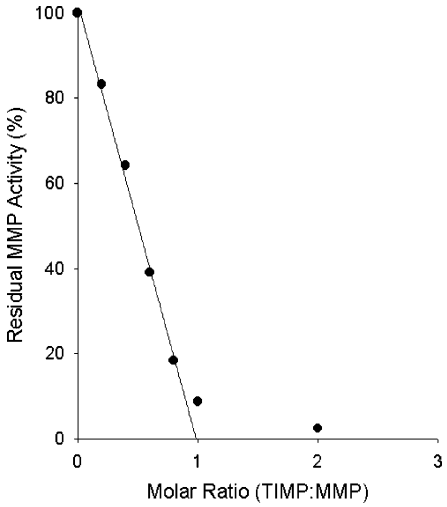

FIGURE 2: Titration of MMP-3(ΔC) by dN-TIMP. Different concentrations of dN-TIMP (0−400 nM) were mixed with 200 nM MMP-3(ΔC) and incubated at room temperature overnight. The residual MMP-3 activity was measured using the synthetic substrate NFF-3.

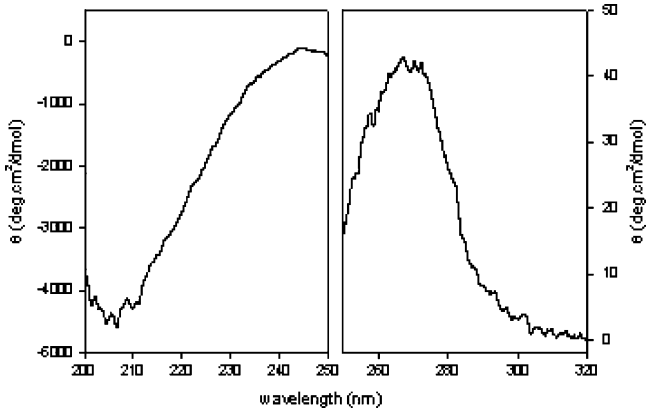

FIGURE 3: Near-UV (right) and far-UV (left) CD spectra of recombinant dN-TIMP. The protein was dialyzed against 10 mM MES (pH 6.0) containing 50% glycerol, and both CD spectra were determined as averages of 10 scans at 30 °C with a JASCO J-600 spectropolarimeter. Near-UV CD spectra were recorded at a protein concentration of 0.3 mg/mL using a cell with a path length of 1 cm, and far-UV spectra were recorded at a protein concentration of 0.15 mg/mL using a cell with a path length of 0.1 cm.

produced as described here, appears to be higher than previously reported (*23*) since it could be continuously monitored by fluorimetry at an enzyme concentration of 10 nM (Figure 4A), whereas in previous studies, incubation of 20 nM enzyme with fluorogenic substrate for 16 h was required to obtain a useful activity measurement (*23*). However, the activity of *dm2*-MMP with Knight substrate was low as in previous studies (*24*) and was determined by single-point assays at an enzyme concentration of 100 nM.

dN-TIMP Is an Endogenous Inhibitor of Both Drosophila MMPs. Both *Drosophila* MMPs cleave the synthetic peptide substrate Knight, but at rates lower than those of human MMPs. Substrate cleavage by *dm1*-MMP was strongly inhibited by dN-TIMP with an apparent $K_i^{(app)}$ of 2.3 ± 0.9 nM (Figure 4). Because of its lower activity, the inhibition of *dm2*-MMP could only be determined at an enzyme concentration of 100 nM, precluding the determination of K_i values in the low nanomolar range. At 100 nM, *dm2*-MMP was inhibited 49% after preincubation with 100 nM

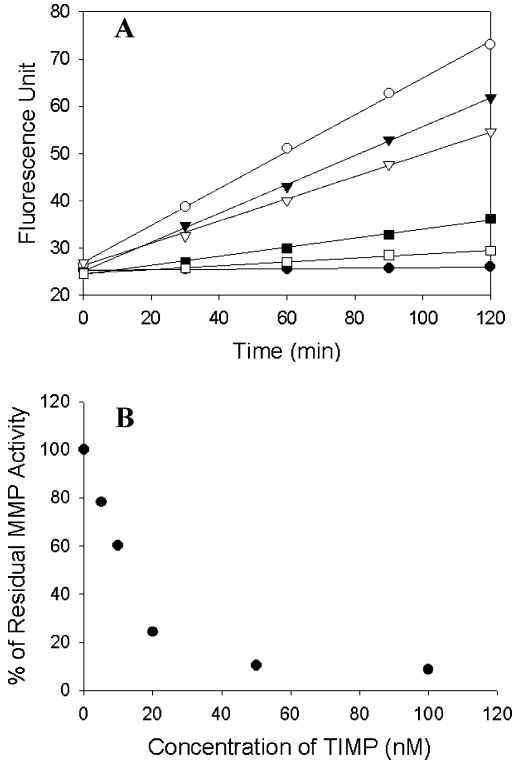

FIGURE 4: Inhibition of *dm1*-MMP by dN-TIMP. Activated *dm1*-MMP was preincubated at room temperature for 2 h with 0−100 nM dN-TIMP, followed by addition of Knight substrate and incubation for an additional 2 h. The fluorescence intensity was measured every 30 min. (A) Kinetics of uninhibited and inhibited *dm1*-MMP: (●) 0 nM *dm1*-MMP, (○) 10 nM *dm1*-MMP, (▼) 10 nM *dm1*-MMP and 5 nM dN-TIMP, (▽) 10 nM *dm1*-MMP and 10 nM dN-TIMP, (■) 10 nM *dm1*-MMP and 20 nM dN-TIMP, and (□) 10 nM *dm1*-MMP and 50 nM dN-TIMP. (B) Data from panel A replotted to show the dose-dependent inhibition of *dm1*-MMP by dN-TIMP.

Table 1: Inhibition Constants, $K_i^{(app)}$, of dN-TIMP and N-TIMP-3 for Some Human MMPs and ADAMs[a]

	$K_i^{(app)}$ (nM)	
metzincin	dN-TIMP	N-TIMP-3
MMP-1	31 ± 5	1.2 ± 0.5[b]
MMP-2	7.7 ± 0.7	4.3 ± 0.5[b]
MMP-3(ΔC)	0.3 ± 0.03	67 ± 3[b]
MT1-MMP(CD)	14 ± 1	0.8 ± 0.03
TACE	0.6 ± 0.04	9.6 ± 0.5
ADAM10	106 ± 10	74 ± 6

[a] Concentrations of enzymes used in the assays: 5 nM MMP-1, 1 nM MMP-2, 1 nM MMP-3(ΔC), 5 nM MT1-MMP(CD), 0.14 nM TACE (ectodomain), and 19.2 nM ADAM10 (ectodomain). [b] Data taken from ref *15*.

dN-TIMP, and 71% with 200 nM dN-TIMP. These results suggest that dN-TIMP is an inhibitor of both *Drosophila* MMPs, but its $K_i^{(app)}$ value for *dm2*-MMP is on the order of 100 nM, much higher than for *dm1*-MMP.

Inhibition of Human MMPs and ADAMs by dN-TIMP. As shown in Table 1, human MMP-1−3 and -14 (MT1-MMP) are inhibited by dN-TIMP. Unlike N-TIMP-3, which has a low K_i for collagenase 1 (MMP-1) and a much weaker affinity for stromelysin 1 (MMP-3), *Drosophila* N-TIMP is a very good inhibitor of MMP-3 but is less effective with MMP-1 (Table 1). Interestingly, dN-TIMP is also a good inhibitor of MT1-MMP(CD), with a $K_i^{(app)}$ of 14 nM (Table 1). MT1-MMP is effectively inhibited by N-TIMP-2−4 but not by N-TIMP-1 (*7*−*10*).

dN-TIMP was tested for its inhibitory activity against two human ADAMs, TACE/ADAM17 and ADAM10. We observed very strong inhibition of the proteolytic activity of the ectodomain of human TACE for cleavage of a synthetic substrate, with an apparent K_i of 0.6 nM (Table 1). However, inhibition of the activity of the ectodomain of human ADAM10 by dN-TIMP was much weaker with a $K_i^{(app)}$ of 106 nM. Human N-TIMP-3 is also a better inhibitor for TACE than ADAM10, but the selectivity is lower than that of dN-TIMP [$K_i^{(app)}$ = 9.6 nM for TACE and 74 nM for ADAM10 (Table 1)].

Structural Models for dN-TIMP and N-TIMP-3 Reveal a Similarity in Surface Charge Distribution. Comparison of the crystal structures of free and bound TIMP-2 shows relatively small conformational changes in the N-terminal domain of the TIMP upon binding to the MMP, except for the A−B loop which is much shorter in TIMP-3 (*6*). Both models of dN-TIMP and N-TIMP-3 were generated on the basis of the published structures of TIMP-1 and TIMP-2 in complexes with MMPs (*34*, *35*), and are therefore models of the bound states of these TIMPs. The structural model of dN-TIMP is less similar to the experimentally determined structures of TIMP-1 and TIMP-2 than the model of N-TIMP-3, reflecting a lower level of sequence identity and a lack of the third disulfide bond. However, the two models are strikingly similar in surface charge distribution (Figure 5). The region around the reactive site of both inhibitors has a preponderance of negatively charged residues, mostly located in the C−D loop (Figure 5A,C). On the opposite face of the molecules there is a large continuous surface of positive charge, mostly contributed by residues within strands A and B, the B−C loop, and α-helix 3 (Figure 5B,D). In contrast, the surface charge in TIMP-1 and TIMP-2 is more evenly distributed (not shown).

DISCUSSION

In this paper, we described a method for preparing a fully active form of the inhibitory domain of *Drosophila* TIMP (dN-TIMP), and its properties as an inhibitor of MMPs and ADAMs. A unique feature of dN-TIMP is that it contains only two of the three disulfide bonds that are present in the inhibitory domains of all other currently known TIMPs (*6*). Previously, variants of TIMP-1 with substitutions for Cys^{13} or Cys^{124}, or with a truncation at Cys^{124}, were not found in the culture medium in a HeLa cell expression system (*39*), suggesting that the Cys^{13}−Cys^{124} disulfide is structurally important. However, the high inhibitory activity of dN-TIMP for multiple metzincins indicates that the missing disulfide bond, which corresponds to the Cys^{13}−Cys^{124} disulfide in TIMP-1, is not necessary for the structure or inhibitory activity of N-TIMPs.

Recombinant dN-TIMP inhibits all four human MMPs that were tested. Its relatively weak inhibition of MMP-1 and potent inhibition of MMP-3 are consistent with its reactive site structure and previous mutational studies with N-TIMP-1 (*33*, *40*). dN-TIMP has Ser as residue 2 and Met as residue 4, and a T2S mutation in N-TIMP-1 weakens binding to MMP-1 while enhancing binding to MMP-3 (*40*); also, a bulky side chain in position 4 (i.e., Met) weakens binding

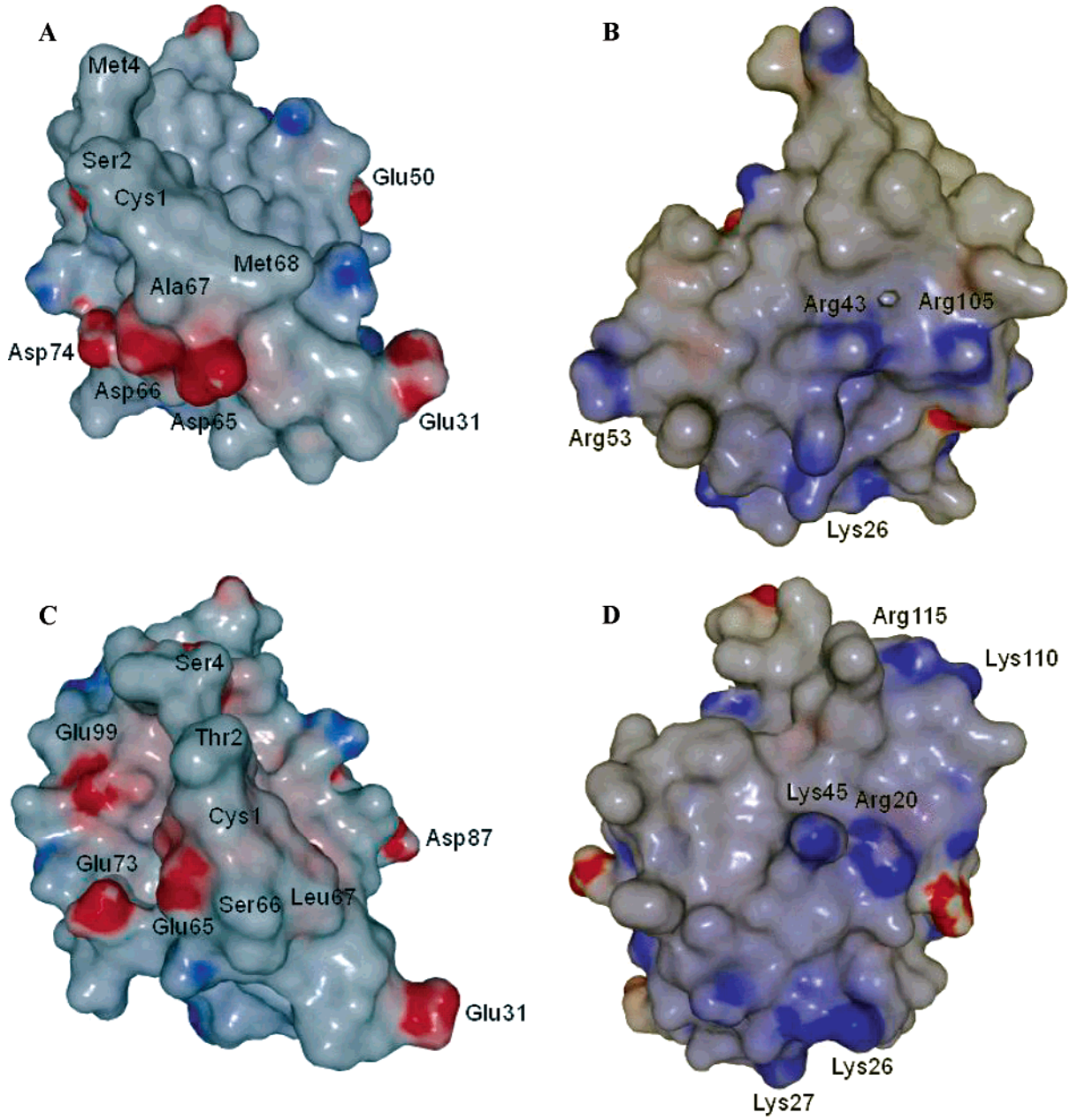

FIGURE 5: Structural models of dN-TIMP and N-TIMP-3. Models were built on the basis of the structures of TIMP-1 and TIMP-2, using the Homology module of Insight II. Solid surface structures of dN-TIMP and N-TIMP-3 were displayed using GRASP (*34*), with the negatively charged surface colored red and the positively charged surface colored blue: (A) dN-TIMP (front), (B) dN-TIMP (back), (C) N-TIMP-3 (front), and (D) N-TIMP-3 (back), where front refers to the surface surrounding the MMP binding site and back refers to the reverse surface.

to MMP-1 (*33*). The relatively low activity of dN-TIMP against MMP-1, the only collagenase tested in this study, may reflect an adaptation to the different ECM compositions of *Drosophila* and vertebrates. The *Drosophila* genome is devoid of genes for fibrillar collagens (*25*), molecules that are the exclusive targets of collagenases. Thus, dN-TIMP would not be under selective pressure to acquire or maintain features required for effective collagenase inhibition. Unlike N-TIMP-1, which interacts weakly with the membrane-type MMPs, dN-TIMP inhibits MT1-MMP with an apparent K_i of 14 nM. The difference between TIMP-1 and TIMP-2 in inhibitory activity for MT1-MMP has been attributed to the A−B loop, which is elongated in TIMP-2 and allows extra interaction with MT1-MMP (*41*, *42*). However, in N-TIMP-3 and dN-TIMP, both of which inhibit MT1-MMP effectively, the A−B loop is similar in size to that of N-TIMP-1. Therefore, some other structural element in TIMPs must contribute to the binding affinity for MT1-MMP, at least in the cases of N-TIMP-3 and dN-TIMP.

The catalytic domains of *dm1*- and *dm2*-MMPs, the only MMPs present in *Drosophila*, are also inhibited by dN-TIMP. Structurally, this is not unexpected since both *Drosophila* MMPs are closely related to the mammalian MT-MMPs; like MT-MMPs, *dm1*-MMP was shown to be efficiently inhibited by TIMP-2 and -4 but not TIMP-1 (*23*, *24*). Most recently, Page-McCaw *et al*. showed that coexpression of *Timp* in *Drosophila* could suppress phenotypes caused by misexpression (overexpression in incorrect tissues) of *Mmp* genes, and that misexpression of *Timp* mimics the *dm1-Mmp* mutant phenotype (*43*). These results, together with our *in*

vitro data, strongly suggest that the inhibition of endogenous MMPs, particularly *dm1*-MMP, is at least part of the function of TIMP in *Drosophila*.

Studies on *Mmp*-null flies indicate that *dm1*-MMP is essential for the development of the larval tracheal system, *dm2*-MMP is essential for the fusion of the wing imaginal tissue and required for histolysis of larval tissues, while both MMPs appear to have important roles in pupal head eversion (*43*). However, no native substrate in *Drosophila* has been identified so far for these two MMPs.

dN-TIMP is a potent inhibitor of human TACE with an apparent K_i at the sub-nanomolar level, even lower than that of N-TIMP-3, the only TIMP known to inhibit TACE efficiently (Table 1). Interestingly, the presence of Met^4 in dN-TIMP is consistent with the observation that a Ser^4 to Met mutation in N-TIMP-3 enhances its affinity for TACE (*44*). dN-TIMP also inhibits human ADAM10, the only other member of the ADAM family whose sequence is highly similar with that of TACE (*45*), although the binding is more than 170-fold weaker than with TACE. Thus, *Drosophila* N-TIMP represents an ADAM inhibitor that is more selective for TACE, in contrast with human N-TIMP-1, which is selective for ADAM10 (*11*).

Several ADAM genes have been identified in *D. melanogaster*, including the *Drosophila* Kuzbanian/ADAM10 gene. Recently, we identified a *Drosophila* EST clone containing the complete coding sequence for TACE (GenBank entry AY212802). The deduced amino acid sequence for the encoded protein is 41% identical to that of human TACE. The most conserved region is the catalytic domain, which is 49% identical between these two species (alignment not shown). Since the binding of TIMP-3 to TACE is primarily through the interaction of the catalytic domain of TACE with the inhibitory domain of TIMP (*16*, *17*), it is likely that *Drosophila* TIMP can also inhibit the *Drosophila* TACE. Thus, the sole TIMP in fruit flies appears to be an endogenous inhibitor of ADAMs as well as MMPs.

Surface electrostatic potential is known to make a key contribution to the functional properties of proteins that engage in protein−protein interactions (*46*). Long-range electrostatic interactions can steer associating proteins into an appropriate orientation for effective complex formation, thereby enhancing on-rates for their interaction and increasing the equilibrium association constants (*47*). Electrostatic steering is particularly affected by residues at the periphery of the protein−protein interaction sites (*47*). Comparisons of electrostatic surface potentials between sets of proteins appear to be effective for identifying similarities in function (reviewed in ref *48*). It is therefore significant that the structural models of the bound forms of dN-TIMP and N-TIMP-3 are similar in surface electrostatic potential, but distinct from N-TIMP-1 and N-TIMP-2. The surfaces of dN-TIMP and N-TIMP-3 in the vicinity of the MMP-binding ridge contain a cluster of negatively charged residues, which may influence the affinity and selectivity for MMPs. The opposite faces of the two models contain a large positively charged area. Although this could facilitate orienting the inhibitors for an initial interaction with the catalytic domain of TACE, which has a slightly anionic surface with an "acidic" protuberance (*49*), this seems to be inconsistent with a mechanism of inhibition resembling that for MMPs. Yu and co-workers (*50*) have proposed that the cationic A and B strands are responsible for the binding of TIMP-3 to ECM, a unique feature of this inhibitor, presumably by interacting with heparan sulfate and other sulfated glycosaminoglycans. The surface similarity with N-TIMP-3 suggests that *Drosophila* TIMP may also bind to the ECM.

As discussed above, N-TIMP-3 is the most similar to dN-TIMP among human N-TIMPs, because that they have the highest level of sequence identity and similar surface charge pattern and functional properties, particularly the ability to inhibit MT1-MMP, TACE, and ADAM10. Previous studies have shown that *Timp-3*-null mice have spontaneous air space enlargement in the lungs (*51*). In *Drosophila*, mutants misexpressing *Timp* exhibit stretched tracheal systems and tracheal defects during the larval stages (*43*), indicating that both *Drosophila* TIMP and mammalian TIMP-3 play important roles in the development of the respiratory system. In the gene duplication model for vertebrate evolution (*52*), the four mammalian TIMP genes evolved from a common ancestor through a 4-fold amplification of large portions of the genome (*18*, *21*); the theory of subfunctionalization also hypothesizes that duplicated genes experience degenerative mutations that cause losses of subfunctions so that the functions of the ancestral gene are partitioned among the duplicates (*21*, *53*, *54*). A possible example of this process is the recent report that substitution of Thr^{98} with leucine transforms TIMP-1 into an active inhibitor for MT1-MMP (*55*), indicating that TIMP-1 may have lost this subfunction through a single degenerative mutation. TIMP-4 is expressed predominantly in heart (*56*), suggesting one or more unique tissue-specific subfunctions of this gene. However, the evolution of the TIMPs is convoluted by an increased array of targets, the MMPs and ADAMs, in vertebrates and also by their roles in cell proliferation, which may be independent of metalloproteinase inhibition (*6*). It is therefore interesting that our results show that the single *Drosophila* TIMP is most similar to mammalian TIMP-3 in structure and function. This suggests that TIMP-3 may have preserved most of the functions of the ancestral gene because its selective pressure was greater than that of its mammalian counterparts during evolution, and that the other three paralogues have diverged more extensively through mutational changes. Previous work shows that MMPs from *Drosophila* and *C. elegans* can be inhibited by human TIMPs (*23*, *57*). Here we show that the *Drosophila* TIMP can inhibit both human MMPs and ADAMs. These data highlight the conservation of the structures and functions of metzincins and TIMPs from invertebrates to mammals.

ACKNOWLEDGMENT

We thank Dr. Theodore E. Haerry for a gift of the *Drosophia* embryonic cDNA library and Dr. Hideaki Nagase for kindly providing us with the human MMPs. We also thank Drs. Yingnan Zhang, Shalini Iyer, and K. Ravi Acharya for their help in building the structural models of dN-TIMP and N-TIMP-3 and in generating Figure 5.

REFERENCES

1. Nagase, H., and Woessner, J. F., Jr. (1999) *J. Biol. Chem. 274*, 21491−21494.
2. Woessner, J. F., Jr. (2002) *Mol. Biotechnol. 22*, 33−49.
3. Primakoff, P., and Myles, D. G. (2000) *Trends Genet. 16*, 83−87.

4. Bode, W., Gomis-Ruth, F. X., and Stockler, W. (1993) *FEBS Lett. 331*, 134−140.
5. Moss, M. L., White, J. M., Lambert, M. H., and Andrews, R. C. (2001) *Drug Discovery Today 6*, 417−426.
6. Brew, K., Dinakarpandian, D., and Nagase, H. (2000) *Biochim. Biophys. Acta 1477*, 267−283.
7. Will, H., Atkinson, S. J., Butler, G. S., Smith, B., and Murphy, G. (1996) *J. Biol. Chem. 271*, 17119−17123.
8. Bigg, H. F., Morrison, C. J., Butler, G. S., Bogoyevitch, M. A., Wang, Z., Soloway, P. D., and Overall, C. M. (2001) *Cancer Res. 61*, 3610−3618.
9. Butler, G. S., Will, H., Atkinson, S. J., and Murphy, G. (1997) *Eur. J. Biochem. 244*, 653−657.
10. Shimada, T., Nakamura, H., Ohuchi, E., Fujii, Y., Murakami, Y., Sato, H., Seiki, M., and Okada, Y. (1999) *Eur. J. Biochem. 262*, 907−914.
11. Amour, A., Knight, C. G., Webster, A., Slocombe, P. M., Stephens, P. E., Knauper, V., Docherty, A. J., and Murphy, G. (2000) *FEBS Lett. 473*, 275−279.
12. Loechel, F., Fox, J. W., Murphy, G., Albrechtsen, R., and Wewer, U. M. (2000) *Biochem. Biophys. Res. Commun. 278*, 511−515.
13. Amour, A., Slocombe, P. M., Webster, A., Butler, M., Knight, C. G., Smith, B. J., Stephens, P. E., Shelley, C., Hutton, M., Knauper, V., Docherty, A. J., and Murphy, G. (1998) *FEBS Lett. 435*, 39−44.
14. Hashimoto, G., Aoki, T., Nakamura, H., Tanzawa, K., and Okada, Y. (2001) *FEBS Lett. 494*, 192−195.
15. Kashiwagi, M., Tortorella, M., Nagase, H., and Brew, K. (2001) *J. Biol. Chem. 276*, 12501−12504.
16. Lee, M. H., Knauper, V., Becherer, J. D., and Murphy, G. (2001) *Biochem. Biophys. Res. Commun. 280*, 945−950.
17. Lee, M. H., Verma, V., Maskos, K., Becherer, J. D., Knauper, V., Dodds, P., Amour, A., and Murphy, G. (2002) *FEBS Lett. 520*, 102−106.
18. Pohar, N., Godenschwege, T. A., and Buchner, E. (1999) *Genomics 57*, 293−296.
19. Montagnani, C., Le Roux, F., Berthe, F., and Escoubas, J. M. (2001) *FEBS Lett. 500*, 64−70.
20. Rahkonen, O. P., Koskivirta, I. M., Oksjoki, S. M., Jokinen, E., and Vuorio, E. I. (2002) *Biochim. Biophys. Acta 1577*, 45−52.
21. Yu, W. P., Brenner, S., and Venkatesh, B. (2003) *Trends Genet. 19*, 180−183.
22. Godenschwege, T. A., Pohar, N., Buchner, S., and Buchner, E. (2000) *Eur. J. Cell Biol. 79*, 495−501.
23. Llano, E., Pendas, A. M., Aza-Blanc, P., Kornberg, T. B., and Lopez-Otin, C. (2000) *J. Biol. Chem. 275*, 35978−35985.
24. Llano, E., Adam, G., Pendas, A. M., Quesada, V., Sanchez, L. M., Santamaria, I., Noselli, S., and Lopez-Otin, C. (2002) *J. Biol. Chem. 277*, 23321−23329.
25. Hynes, R. O., and Zhao, Q. (2000) *J. Cell Biol. 150*, F89−F96.
26. Pan, D., and Rubin, G. M. (1997) *Cell 90*, 271−280.
27. Qi, H., Rand, M. D., Wu, X., Sestan, N., Wang, W., Rakic, P., Xu, T., and Artavanis-Tsakonas, S. (1999) *Science 283*, 91−94.
28. Rooke, J., Pan, D., Xu, T., and Rubin, G. M. (1996) *Science 273*, 1227−1231.
29. Klein, T. (2002) *Dev. Genes Evol. 212*, 251−255.
30. Fambrough, D., Pan, D., Rubin, G. M., and Goodman, C. S. (1996) *Proc. Natl. Acad. Sci. U.S.A. 93*, 13233−13238.
31. Huang, W., Suzuki, K., Nagase, H., Arumugam, S., Van Doren, S. R., and Brew, K. (1996) *FEBS Lett. 384*, 155−161.
32. Butler, G. S., Hutton, M., Wattam, B. A., Williamson, R. A., Knauper, V., Willenbrock, F., and Murphy, G. (1999) *J. Biol. Chem. 274*, 20391−20396.
33. Wei, S., Chen, Y., Chung, L., Nagase, H., and Brew, K. (2003) *J. Biol. Chem. 278*, 9831−9834.
34. Gomis-Ruth, F. X., Maskos, K., Betz, M., Bergner, A., Huber, R., Suzuki, K., Yoshida, N., Nagase, H., Brew, K., Bourenkov, G. P., Bartunik, H., and Bode, W. (1997) *Nature 389*, 77−81.
35. Fernandez-Catalan, C., Bode, W., Huber, R., Turk, D., Calvete, J. J., Lichte, A., Tschesche, H., and Maskos, K. (1998) *EMBO J. 17*, 5238−5248.
36. Nicholls, A., Sharp, K. A., and Honig, B. (1991) *Proteins 11*, 281−296.
37. Arumugam, S., Gao, G., Patton, B. L., Semenchenko, V., Brew, K., and Van Doren, S. R. (2003) *J. Mol. Biol. 327*, 719−734.
38. Troeberg, L., Tanaka, M., Wait, R., Shi, Y. E., Brew, K., and Nagase, H. (2002) *Biochemistry 41*, 15025−15035.
39. Caterina, N. C., Windsor, L. J., Yermovsky, A. E., Bodden, M. K., Taylor, K. B., Birkedal-Hansen, H., and Engler, J. A. (1997) *J. Biol. Chem. 272*, 32141−32149.
40. Meng, Q., Malinovskii, V., Huang, W., Hu, Y., Chung, L., Nagase, H., Bode, W., Maskos, K., and Brew, K. (1999) *J. Biol. Chem. 274*, 10184−10189.
41. Williamson, R. A., Carr, M. D., Frenkiel, T. A., Feeney, J., and Freedman, R. B. (1997) *Biochemistry 36*, 13882−13889.
42. Williamson, R. A., Hutton, M., Vogt, G., Rapti, M., Knauper, V., Carr, M. D., and Murphy, G. (2001) *J. Biol. Chem. 276*, 32966−32970.
43. Page-McCaw, A., Serano, J., Sante, J. M., and Rubin, G. M. (2003) *Dev. Cell 4*, 95−106.
44. Lee, M. H., Verma, V., Maskos, K., Nath, D., Knauper, V., Dodds, P., Amour, A., and Murphy, G. (2002) *Biochem. J. 364*, 227−234.
45. Moss, M. L., Jin, S. L., Milla, M. E., Bickett, D. M., Burkhart, W., Carter, H. L., Chen, W. J., Clay, W. C., Didsbury, J. R., Hassler, D., Hoffman, C. R., Kost, T. A., Lambert, M. H., Leesnitzer, M. A., McCauley, P., McGeehan, G., Mitchell, J., Moyer, M., Pahel, G., Rocque, W., Overton, L. K., Schoenen, F., Seaton, T., Su, J. L., Becherer, J. D., *et al*. (1997) *Nature 385*, 733−736.
46. Janin, J. (1997) *Proteins 28*, 153−161.
47. Marvin, J. S., and Lowman, H. B. (2003) *Biochemistry 42*, 7077−7083.
48. Blomberg, N., Gabddoulline, R. R., Nilges, M., and Wade, R. C. (1999) *Proteins 37*, 379−387.
49. Maskos, K., Fernandez-Catalan, C., Huber, R., Bourenkov, G. P., Bartunik, H., Ellestad, G. A., Reddy, P., Wolfson, M. F., Rauch, C. T., Castner, B. J., Davis, R., Clarke, H. R., Petersen, M., Fitzner, J. N., Cerretti, D. P., March, C. J., Paxton, R. J., Black, R. A., and Bode, W. (1998) *Proc. Natl. Acad. Sci. U.S.A. 95*, 3408−3412.
50. Yu, W. H., Yu, S., Meng, Q., Brew, K., and Woessner, J. F., Jr. (2000) *J. Biol. Chem. 275*, 31226−31232.
51. Leco, K. J., Waterhouse, P., Sanchez, O. H., Gowing, K. L., Poole, A. R., Wakeham, A., Mak, T. W., and Khokha, R. (2001) *J. Clin. Invest. 108*, 817−829.
52. Aparicio, S. (1998) *Nat. Genet. 18*, 301−303.
53. Force, A., Lynch, M., Pickett, F. B., Amores, A., Yan, Y. L., and Postlethwait, J. (1999) *Genetics 151*, 1531−1545.
54. Lynch, M., and Force, A. (2000) *Genetics 154*, 459−473.
55. Lee, M. H., Rapti, M., and Murphy, G. (2003) *J. Biol. Chem.* (in press).
56. Greene, J., Wang, M., Liu, Y. E., Raymond, L. A., Rosen, C., and Shi, Y. E. (1996) *J. Biol. Chem. 271*, 30375−30380.
57. Wada, K., Sato, H., Kinoh, H., Kajita, M., Yamamoto, H., and Seiki, M. (1998) *Gene 211*, 57−62.

BI035358X